HHS Public Access

Author manuscript

J Bone Miner Res. Author manuscript; available in PMC 2020 August 01.

Published in final edited form as:

J Bone Miner Res. 2019 August ; 34(8): 1407–1418. doi:10.1002/jbmr.3729.

Independent Roles of Estrogen Deficiency and Cellular Senescence in the Pathogenesis of Osteoporosis: Evidence in Young Adult Mice and Older Humans

Joshua N. Farr, Ph.D.[*], **Jennifer L. Rowsey, B.S.**, **Brittany A. Eckhardt, B.S.**, **Brianne S. Thicke, M.S.**, **Daniel G. Fraser, Ph.D.**, **Tamar Tchkonia, Ph.D.**, **James L. Kirkland, M.D., Ph.D.**, **David G. Monroe, Ph.D.**, **Sundeep Khosla, M.D.**[*]

Robert and Arlene Kogod Center on Aging and Division of Endocrinology, Mayo Clinic College of Medicine, Rochester, MN, 55905

Abstract

Estrogen deficiency is a seminal mechanism in the pathogenesis of osteoporosis. Mounting evidence, however, establishes that cellular senescence, a fundamental mechanism that drives multiple age-related diseases, also causes osteoporosis. Recently, we systematically identified an accumulation of senescent cells, characterized by increased $p16^{Ink4a}$ and $p21^{Cip1}$ levels and development of a senescence-associated secretory phenotype (SASP), in mouse bone/marrow and human bone with aging. We then demonstrated that elimination of senescent cells prevented age-related bone loss using multiple approaches, *e.g.,* treating old mice expressing a "suicide" transgene, *INK-ATTAC*, with AP20187 to induce apoptosis of $p16^{Ink4a}$-senescent cells or periodically treating old wild-type mice with "senolytics" – *i.e.,* drugs that eliminate senescent cells. Here, we investigate a possible role for estrogen in the regulation of cellular senescence using multiple approaches. First, sex steroid deficiency two-months post ovariectomy (OVX, n=15) or orchidectomy (ORCH, n=15) *versus* sham surgery (SHAM, n=15/sex) in young adult (4-month-old) wild-type mice did not alter senescence biomarkers or induce a SASP in bone. Next, in elderly postmenopausal women, three weeks of estrogen therapy (n=10; 74±5 yrs) as compared to no treatment (n=10; 78±5 yrs) did not alter senescence biomarkers or induce a SASP in human bone biopsies. Finally, young adult (4-month-old) female *INK-ATTAC* mice were randomized (n=17/group) to SHAM+Vehicle, OVX+Vehicle, or OVX+AP20187 for two months. As anticipated, OVX+Vehicle caused significant trabecular/cortical bone loss as compared to SHAM +Vehicle. However, treatment with AP20187, which eliminates senescent cells in *INK-ATTAC* mice, did not rescue the OVX-induced bone loss or alter senescence biomarkers. Collectively, our

[*]**Co-corresponding authors:** Joshua N. Farr, Ph.D., Guggenheim 7, Mayo Clinic College of Medicine, 200 First Street SW, Rochester, Minnesota 55905; Tel. +1-507-538-0085; farr.joshua@mayo.edu, Sundeep Khosla, M.D., Mayo Clinic College of Medicine, 200 First Street SW, Rochester, Minnesota 55905; Tel: 507-255-6663; khosla.sundeep@mayo.edu.

Author contributions: J.N.F. and S.K. conceived and directed the project with input from T.T., J.L.K, and D.G.M. J.N.F. and S.K. designed the experiments and interpreted the data. Experiments were performed by J.N.F, J.L.R, B.A.E., B.S.T., and D.G.F. J.N.F. wrote the manuscript. All authors reviewed the manuscript. J.N.F. and S.K. oversaw all experimental design, data analyses, and manuscript preparation. J.N.F. and S.K. accept responsibility for the integrity of the data analysis.

Supplementary Material: This manuscript contains Supplementary Information and Figures

Disclosures: T.T. and J.L.K. have a financial interest related to this research. Patents on *INK-ATTAC* mice and senolytic drugs are held by Mayo Clinic. This research has been reviewed by the Mayo Clinic Conflict of Interest Review Board and was conducted in compliance with Mayo Clinic Conflict of Interest policies. No other authors have a relevant financial conflict of interest.

data establish independent roles of estrogen deficiency and cellular senescence in the pathogenesis of osteoporosis, which has important implications for testing novel senolytics for skeletal efficacy, as these drugs will need to be evaluated in preclinical models of aging as opposed to the current FDA model of prevention of OVX-induced bone loss.

Keywords

aging; bone; osteocyte; sex steroids; estrogen therapy; osteoporosis; animal models

Introduction

The decline in gonadal estrogen production during the menopause in women or the reduction in bioavailable estrogen levels with aging in men contributes to age-related bone loss and an increased fracture risk.[1,2] Indeed, seminal observations made by Fuller Albright dating back many years ago[3] establish that estrogen has a crucial impact on bone metabolism as its decline is causal in the pathogenesis of osteoporosis. More definitive evidence supporting these initial observations came from the Women's Health Initiative (WHI), which clearly established that estrogen therapy has anti-fracture efficacy.[4] However, this study also revealed multiple adverse effects of estrogen therapy on non-skeletal tissues,[4] eventually leading to the diminished use of estrogen therapy clinically as a viable option for osteoporosis prophylaxis.[5] Nevertheless, insights into the mechanisms of estrogen regulation of bone metabolism could still lead to novel drug targets for more effective prevention and treatment of osteoporosis.[6] Moreover, because Food and Drug Administration (FDA) guidelines recommend the use of ovariectomy (OVX) as a standard preclinical animal model to demonstrate the efficacy and safety of new drugs for osteoporosis therapy,[7] it is important to determine the extent to which this model recapitulates our expanding knowledge of the spectrum of fundamental mechanisms contributing to organismal skeletal aging.[8] Indeed, while bone loss in humans occurs both in response to estrogen deficiency and in the setting of aging, the underlying mechanisms responsible for causing bone loss during these periods need to be understood so novel strategies can be developed to target those specific mechanisms and tailor personalized therapy to patients in a context-specific manner.

While estrogen deficiency has clearly been established as seminal mechanism in the pathogenesis of osteoporosis, recent mounting evidence demonstrates that cellular senescence, a fundamental mechanism that drives multiple age-related diseases,[9] also drives bone loss with aging. Indeed, in the setting of old age, our group systematically identified senescent cells in the bone microenvironment,[10] and demonstrated a causal role for senescent cells in mediating age-related bone loss.[11] In mice, we found that expression of the key mediator of cellular senescence, $p16^{Ink4a}$ (encoded by the Ink4a/Arf locus, also known as *Cdkn2a*),[9] increased *in vivo* with aging in enriched populations of myeloid cells, B- and T-cells, osteoprogenitors, osteoblasts, and osteocytes; the latter finding is consistent with observations by Piemontese and colleagues.[12] In our study,[10] we confirmed an accumulation of senescent osteocytes in old bone using an established *in vivo* biomarker of senescence – *i.e.* the senescence-associated distention of satellites (SADS) assay,[13] which

is a measure of higher-order unfolding of satellite DNA heterochromatin characteristic of senescent cells. We also found that expression of *p21*^{Cip1} (*Cdkn1a*), a cell cycle inhibitor downstream of p53 that also drives senescence,[9] was increased with aging in osteocyte-enriched bone samples from males, but not females.[10] Interestingly, Kim and colleagues[14] have reported that osteoprogenitors isolated from old Osx1-Cre;TdRFP mice exhibited increased *p21*^{Cip1} levels as well as features of the senescence-associated secretory phenotype (SASP). A key signature of the SASP is upregulation of pro-inflammatory chemokines, cytokines, and extracellular matrix-degrading proteins,[15–17] which have been hypothesized to drive age-related dysfunction in multiple tissues.[9] Our group has shown that in addition to senescent myeloid cells, senescent osteocytes are key SASP producers with aging.[10] In addition to these findings in mice, we found similar results in bone biopsies, containing a heterogeneous population of marrow and bone cells, from older relative to younger women, indicating parallel findings in humans.[10] Collectively, these data demonstrate that senescent cells accumulate in the bone microenvironment at the time and location of age-related bone loss in both mice and humans.

Based on this evidence, we hypothesized that eliminating senescent cells or inhibiting the detrimental effects of their SASP would prevent age-related bone loss.[11] To test this hypothesis, we targeted senescent cells in old mice using multiple approaches: clearance using either a genetic approach, *i.e.,* in *INK-ATTAC* (INK-linked apoptosis through targeted activation of caspase) mice containing a "suicide" transgene driven by the *p16*^{Ink4a} promoter[18] or pharmacologically by periodically administering "senolytics"[19] – *i.e.,* drugs that selectively kill senescent cells – to old wild-type mice.[11] In addition, we treated old wild-type mice with a "senomorphic" drug (*i.e.,* the JAK inhibitor – ruxolitinib[20]) to inhibit the SASP.[11] We found that in old (≥20 months) mice with established bone loss, each of these approaches for 2–4 months improved bone mass and microarchitecture, with the beneficial effects of targeting senescent cells resulting from reduced bone resorption and enhanced bone formation particularly on endocortical surfaces.[11] Therefore, drugs that selectively target senescent cells may represent a novel strategy for the prevention and treatment of osteoporosis. However, prior to testing the potential efficacy and safety of these drugs in OVX preclinical animal models, as recommended by the FDA,[21] we sought in the current study to investigate a possible direct role for estrogen in the regulation of cellular senescence in both young adult mice and older humans.

Support for a potential interaction between sex steroid deficiency and cellular senescence comes from evidence suggesting that premature ovarian dysfunction causes accelerated decline in physical and cognitive functions.[22,23] Indeed, bilateral oophorectomy in animals and humans causes premature loss of ovarian hormones, predominantly estrogen, and leads to multimorbidity, frailty, and the accelerated functional decline of several tissues, including bone.[24] However, the question of which specific underlying mechanism(s) drives accelerated aging in response to sex steroid deficiency remains largely unanswered. Because as in other tissues, the skeletal aging process is driven by fundamental non-adaptive mechanisms that are interconnected, linked, and overlap,[8] we focused our primary analyses on cell senescence biomarkers and the SASP in young adult mice that had undergone gonadectomy to avoid the confounding effects of other fundamental aging mechanisms that exist in the context of older age.[25] In additional exploratory analyses, we measured

senescence biomarkers and the SASP in human bone by taking advantage of previous study performed by our group in which bone biopsies were obtained from older postmenopausal women who received either no treatment or estrogen therapy.[26–28]

Materials and Methods

Animals

Both sexes were studied as specified here and in the Figure Legends. Female (n=30) and male (n=30) young adult (4-month-old) C57BL/6 wild-type (WT) mice were studied. More specifically, the four-month-old females of comparable body weights were randomized to undergoing either sham-operated surgery (SHAM, n=15) or ovariectomy (OVX, n=15) and then were sacrificed 8 weeks later (at age 6 months). Similarly, the 4-month-old males of comparable body weights were randomized to undergoing either SHAM (n=15) or orchidectomy (ORCH, n=15) and then were sacrificed 8 weeks later (at age 6 months). Further, from our earlier work reported previously,[10] we used data on young adult (6-month-old) male (n=12) and female (n=15) mice as well as old (24-month-old) male (n=10) and female (n=9) C57BL/6 WT mice obtained from the NIA. Finally, we generated a cohort of young adult (4-month-old) female *INK-ATTAC* mice (n=51). In the experiments described herein, we used *INK-ATTAC* transgenic line 3 – the generation and characterization of which has been described.[18] As detailed previously, *INK-ATTAC* mice were co-developed by the J.M. van Deursen/D. Baker (Mayo Clinic) and J.L. Kirkland/T. Tchkonia (Mayo Clinic) laboratories. A total of 51 four-month-old female *INK-ATTAC* mice of comparable body weights were randomized to one of three groups (n=17/group): 1) SHAM+Vehicle (4% EtOH, 10% PEG-400, 86% Tween); 2) OVX+Vehicle (4% EtOH, 10% PEG-400, 86% Tween); or 3) OVX+AP20187 (B/B homodimerizer, Clontech, USA; 10 mg of AP20187 per kg body mass [drug/body mass]) administered intraperitoneally [i.p.]) twice weekly for 8 weeks; all four-month-old young adult *INK-ATTAC* mice were sacrificed at age 6 months. Note that this dosing regimen has been effective in eliminating senescent cells in old *INK-ATTAC* mice in multiple previous studies.[11,29,30] All mice were housed within a pathogen free, accredited facility under a 12-hour light/dark cycle with constant temperature (23°C), and had access to water and food (standard mouse diet, Lab Diet 5053, St. Louis, MO, USA) *ad libitum*. All animal protocols were approved by the Institutional Animal Care and Use Committee (IACUC), and all experiments were performed in accordance with Mayo Clinic IACUC guidelines.

Mouse assessments of body composition

At baseline, and bi-weekly thereafter, body mass (g) was recorded on all mice. At baseline and study endpoint, body composition (total body lean and fat mass) was assessed in non-anesthetized, conscious mice by quantitative Echo magnetic resonance imaging (EchoMRI-100, Houston, TX, USA) as described.[31] All assessments were performed in a blinded fashion.

Mouse tissue collection and assessments

Following sacrifice, the uterus or seminal vesicles were harvested from female and male mice, respectively; weights were recorded. Connective tissues and skeletal muscle were

removed from harvested vertebrae and femurs. The lumbar vertebrae (L4-L6) and the right femur were fixed in ethanol (EtOH) prior to micro-computed tomography (μCT) imaging (see below). Following imaging and analysis, the non-decalcified right femur was embedded in methylmethacrylate (MMA), and sectioned, followed by immunohistochemistry (IHC) and fluorescent *in situ* hybridization (FISH) – *i.e.,* the SADS assay (see below). Finally, the remaining vertebrae (L3 and up) were used for isolation of osteocyte-enriched bone samples, details of which have been published elsewhere.[10,11] Briefly, muscle/connective tissues were removed from mouse vertebrae, which were minced using a scalpel and then subjected to endotoxin-free collagenase (Liberase; Roche Diagnostics GmbH, Mannheim, Germany) digestion twice for 30 minutes. As demonstrated previously,[10] the remaining cells represent an osteocyte-enriched population used for real-time quantitative polymerase chain reaction (rt-qPCR) analyses (see below).

Real-time quantitative polymerase chain reaction (rt-qPCR) analysis

Targeted gene expression measurements of mRNA levels were performed by rt-qPCR as described.[10,11] Briefly, total RNA was isolated in accordance with manufacturer's protocol using QIAzol Lysis Reagent following by purification with RNeasy Mini Columns (QIAGEN, Valencia, CA, USA). DNase was then used to degrade potentially contaminating genomic DNA with on-column RNase-free DNase solution (QIAGEN, Valencia, CA, USA). Confirmation of RNA quantity/purity was performed using a Nanodrop spectrophotometer (Thermo Scientific, Wilmington, DE, USA). The High-Capacity cDNA Reverse Transcription Kit (Applied Biosystems by Life Technologies, Foster City, CA, USA) was used to perform reverse transcriptase and rt-qPCR was performed with the ABI Prism 7900HT Real Time System (Applied Biosystems, Carlsbad, CA, USA) using either TaqMan (purchased from Thermo Fisher Scientific, USA) or SYBR green (QIAGEN, Valencia, CA, USA). As done previously,[11] mouse TaqMan assays were used to measure enhanced green fluorescent protein (*EGFP*), which is encoded by the *INK-ATTAC* transgene,[18] $p16^{Ink4a}$ (*Cdkn2a*), $p21^{Cip1}$ (*Cdkn1a*), and *p53* (*Trp53*). Similarly, human TaqMan assays (purchased from Thermo Fisher Scientific, USA) were used to measure $p16^{INK4a}$ (*CDKN2A*), $p21^{CIP1}$ (*CDKN1A*), and *p53* (*TP53*). All other genes were measured with SYBR green as the detection method as described;[10] mouse/human primer sequences are provided in Supplementary Tables 1 and 2, respectively. SYBR green primer sequences were designed using Primer Express® Software Version 3.0 (Applied Biosystems, Foster City, CA). Variations in input RNA were normalized using a panel of 5 reference genes (Mouse: *Actb, Hprt, Polr2a, Tbp, Tub1a*; Human: *ACTB, GAPDH, POLR2A, RPL13A, TUBA1A*) from which the 3 most stable reference genes were selected using the geNorm algorithm (http://medgen.ugent.be/~jvdesomp/genorm/),[32,33] followed by the PCR Miner algorithm[34], which was used to adjust for variability in the efficiency of amplification. Within each sample, the median cycle threshold (Ct) for each gene (run in triplicate) was normalized to the geometric mean of the median Ct of the 3 most stable reference genes; the latter was determined by the geNorm algorithm using the following formula: $2^{(\text{reference Ct} - \text{gene of interest Ct})}$. The ΔCt calculated for each gene was used to determine the relative mRNA gene expression changes for each sample. As done previously,[10] genes with Ct values >35 were considered – Not Expressed (NE). Supplementary Tables 1 and 2 provide the primer sequences used in this study.

Senescence-associated distension of satellites (SADS) analysis of senescent osteocytes

The senescence-associated distention of satellites (SADS)[13] assay was performed in a blinded fashion as described[10,11] to measure higher-order unfolding of satellite DNA heterochromatin, a characteristic feature of senescent cells,[13] in osteocytes located in femur diaphysis cortex. Briefly, the non-decalcified right mouse femur was fixed in EtOH, embedded in methylmethacrylate (MMA), sectioned, and subjected to FISH as described.[10,11] Following 4% paraformaldehyde (PFA) crosslinking of bone sections for 20 minutes, sections were washed 3 times (5 minutes each in PBS), and dehydrated in graded (70%, 90%, and 100% – 3 minutes each) EtOH. Bone sections were then briefly dried and then denatured for 10 minutes at 80°C in hybridization buffer: 25mM $MgCl_2$, 70% formamide (Sigma), 0.1M Tris (pH 7.2), 5% blocking reagent (Roche) with 1.0μg/mL of Cy3-labelled (F3002) CENPB-specific (ATTCGTTGGAAACGGGA) peptide nucleic acid (PNA) probe (Panagene Inc., Korea), followed by dark room hybridization for 2 hours at room temperature. Bone sections were then washed and mounted with vectashield DAPI-containing mounting media (Life Technologies, USA). As described,[10,11] confocal microscopy, performed at the Mayo Clinic Microscopy and Cell Analysis Core, was utilized to visualize SADS (*i.e.,* decondensed/elongated centromeres), the number of which in each osteocyte was quantified in a blinded fashion; a senescent osteocyte was defined using the previously established a cut-off of ≥4 SADS per cell.[10,11]

Skeletal phenotyping

All skeletal imaging and subsequent analyses were done in a blinded fashion. As described previously,[10,11] quantitative analysis of the lumbar spine (L4-L6) and femoral mid-shaft diaphysis were performed using the Viva Scan 40 μCT scanner (Scanco Medical AG, Basserdorf, Switzerland) with the following parameters: 55 kVp, 10.5 μm voxel size, 21.5 diameter, 145mA, 300 ms integration time. Trabecular skeletal parameters were assessed at the lumbar spine (200 slices), including trabecular bone volume fraction (BV/TV; %), trabecular number (Tb.N; 1/mm), trabecular thickness (Tb.Th; mm), and trabecular separation (Tb.Sp; mm), while at the femoral mid-diaphysis (50 slices), cortical thickness (Ct.Th; mm), endocortical circumference (E.C; mm), and periosteal circumference (P.C; mm) were derived using the manufacturer's protocols.

Human Subjects

As described,[10,26–28] in a previous study performed by our laboratory we obtained small needle bone biopsies, comprised of both trabecular and cortical bone as well as a heterogeneous population of bone marrow cells (Supplementary Fig. 1),[35] from the posterior iliac crest of healthy younger women (n=10; 26±2 yrs) as well as healthy older female volunteers who received either three weeks of estrogen therapy (100 μg/d of transdermal 17β-estradiol [Alora,Watson Pharma Inc., Corona, CA]; patches were changed every 3–4 days) (n=10; 74±5 yrs) or no treatment (n=10; 78±5 yrs) using an 8G needle under local anesthesia (1% lidocaine) and monitored intravenous sedation. To preserve RNA integrity, the human bone biopsies were immediately homogenized (Tissue Tearor, Cole-Parmer) in lysis buffer (QIAzol; QIAGEN, Valencia, CA, USA) and stored at −80°C until the time of RNA isolation (see rt-qPCR analysis above). Informed written consent was

obtained from all subjects, and all protocols were approved by the Mayo Clinic Institutional Review Board (IRB). Clinical characteristics of the human subjects and their serum biochemistries are provided in Supplementary Table 3. Detailed descriptions of the experimental protocols and study subjects are provided in the Supplementary Methods.

Statistics

Sample sizes were based on previously conducted and published experiments (*e.g.,* Farr et al.[10] and Farr et al.[11]) in which statistically significant differences were observed in μCT-derived skeletal parameters and changes in senescence biomarkers in response to various interventions performed in our laboratory. Investigators were blinded to randomization during experiments and assessments of outcomes. Replicates are noted in the Figure Legends for each separate experiment. Data were checked for normality and distribution using histograms and dot plots; all variables were examined for kurtosis and skewness. No samples were excluded from analyses. Differences between groups were analyzed by independent samples *t*-test, one-way ANOVA, or repeated-measures ANOVA where justified as appropriate (see Figure Legends). Following ANOVA, the Tukey *post-hoc* test was used to adjust for multiple comparisons. Data are presented as Means ± SEM (unless otherwise specified) with $p < 0.05$ (two-tailed) considered statistically significant. Statistical analyses were performed using either Microsoft Excel, GraphPad Prism (Version 6.07), or the Statistical Package for the Social Sciences for Windows, Version 23.0 (SPSS, Chicago, IL). In addition, gene expression data were analyzed using Gene Set Enrichment Analysis (GSEA)[36,37] (http://software.broadinstitute.org/gsea/index.jsp) to determine whether significant gene expression changes occurred in an *a priori* established cluster of 36 established SASP genes, as described previously[10].

Results

In our earlier work, we systematically identified senescent cells in the bone microenvironment with natural chronological aging,[10] and demonstrated a causal role for senescent cells in mediating age-related bone loss in mice.[11] As shown in (Fig. 1A) as previously reported by our group,[10] in osteocyte-enriched bone samples from male WT mice we found by rt-qPCR that mRNA expression of the key mediator of cellular senescence, $p16^{Ink4a}$ (encoded by the Ink4a/Arf locus, also known as *Cdkn2a*)[9] increased with aging (9.9-fold; $p < 0.001$), while $p21^{Cip1}$ (*Cdkn1a*) and p53 (*Trp53*), which can also drive senescence,[9] increased to lesser extent with aging (1.6-fold and 1.5-fold, respectively; $p < 0.01$). To determine whether loss of sex steroids in males induces mediators of cellular senescence in bone (Fig. 1B), we randomized young adult (4-month-old) male C57BL/6 WT mice to undergoing either sham-operated surgery (SHAM, n=15) or orchidectomy (ORCH, n=15); mice were sacrificed 8 weeks later (age 6 months). As shown in Fig. 1C, loss of sex steroids in male WT mice resulted in no detectable changes (all $p > 0.05$) in mRNA levels of mediators of cellular senescence, including $p16^{Ink4a}$, $p21^{Cip1}$, and *p53*, in osteocyte-enriched bone samples as compared to age-matched male WT mice that underwent SHAM. We next compared in male mice how the SASP changed in bone with aging and in response to loss of sex steroids. In our earlier work,[10] we used rt-qPCR to measure the mRNA expression of a panel of 36 established SASP factors in osteocyte-enriched bones samples from young adult

(6-month-old) and old (24-month-old) male WT mice. As shown in Fig. 1D, our previous work[10] demonstrated that mRNA expression of several SASP factors (*i.e.,* 23 of the 36 analyzed; GSEA p-value < 0.001) were significantly increased with aging in osteocyte-enriched bone samples. By contrast, however, loss of sex steroids in young adult (4-month-old) male WT mice resulted in no changes in mRNA expression of the same SASP factors (*i.e.,* none of the 36 were significantly altered; GSEA p-value > 0.05) in osteocyte-enriched bone samples (Fig. 1E).

We next performed rt-qPCR on osteocyte-enriched bone samples from female WT mice to compare age-associated changes in senescence and SASP markers with changes in these same markers in response to estrogen deficiency. In our earlier work,[10] we found that mRNA expression of $p16^{Ink4a}$, but not $p21^{Cip1}$ or *p53*, increased significantly (14.1-fold, $p < 0.001$) with aging in osteocyte-enriched bone samples (Fig. 2A). To determine whether estrogen deficiency in females induces mRNA expression of mediators of cellular senescence in bone (Fig. 2B), we randomized young adult (4-month-old) female WT mice to undergoing either sham-operated surgery (SHAM, n=15) or ovariectomy (OVX, n=15); mice were sacrificed 8 weeks later (age 6 months). Consistent with observations in males, estrogen deficiency in female WT mice resulted in no detectable changes (all $p > 0.05$) in mRNA levels of mediators of cellular senescence, including $p16^{Ink4a}$, $p21^{Cip1}$, and *p53*, in osteocyte-enriched bone samples as compared to age-matched SHAM female WT mice (Fig. 2C). We next used rt-qPCR to measure the mRNA expression of 36 SASP factors in order to compare in female mice how the SASP changed in bone with aging and in response to estrogen deficiency. As shown in Fig. 2D as previously reported by our group,[10] several SASP factors increased significantly with aging (*i.e.,* 18 of the 36 analyzed; GSEA] p-value < 0.001) in osteocyte-enriched bone samples isolated from young adult (6-month-old) *versus* old (24-month-old) female WT mice. By comparison, mRNA expression of relatively few SASP factors (*i.e.,* 5 of 36 analyzed; GSEA p-value > 0.05) increased significantly in osteocyte-enriched bone samples in response to estrogen deficiency, whereas expression of the matrix metalloproteinases, *Mmp3* and *Mmp9*, decreased significantly ($p < 0.05$) (Fig. 2E).

To determine whether our data in mice paralleled those in humans, we next investigated a possible role for estrogen in the regulation of senescence and the SASP in human bone biopsies. To do so, we took advantage of a previous study performed in our laboratory in which we obtained human bone biopsy samples from healthy younger women who received no treatment as well as and older women either receiving either no therapy or treatment with estrogen for three weeks.[28] In order to first establish the efficacy of short-term estrogen therapy on bone turnover, we measured serum levels of bone formation (amino-terminal propeptide of type I collagen; P1NP) and resorption (cross-linked C-telopeptide of type I collagen; CTx) at baseline and after three weeks in the older women. As previously reported,[28] three weeks of estrogen therapy increased serum bone formation levels ($p < 0.001$) and decreased serum bone resorption levels ($p < 0.001$), whereas neither parameter changed in older women who received no therapy over the same time period (Supplementary Table 1). With regards to the human bone biopsies, our previous analysis on this cohort[10] showed by rt-qPCR that mRNA expression of the key mediators of cellular senescence, $p16^{INK4a}$ (*CDKN2A*) and $p21^{CIP1}$ (*CDKN1A*), were significantly increased (both *p-values* < 0.01) in

human bone with aging (Fig. 3A). In the present study, we performed rt-qPCR analysis on the human bone biopsies isolated from older women who received no treatment as compared to older women who received short-term estrogen therapy for 3 weeks (Fig. 3B). Using rt-qPCR, we found that as compared to no treatment, short-term estrogen therapy did not significantly (all $p > 0.05$) alter mRNA levels of senescence mediators, including $p16^{INK4a}$, $p21^{CIP1}$, and *p53* (*TP53*), in human bone (Fig. 3C). Despite the bone biopsies consisting of a heterogeneous population of both bone and marrow cells, our previous analysis[10] detected significant increases in mRNA levels of multiple SASP factors with aging (*i.e.,* 12 of the 36 analyzed; GSEA *p*-value < 0.001) in these samples (Fig. 3D). By contrast, as compared to no treatment, short-term estrogen therapy did not significantly increase the mRNA expression of any of the 36 SASP factors analyzed (GSEA *p*-value > 0.05) in human bone (Fig. 3E).

We next examined whether systemic elimination of senescent cells in young adult mice is sufficient to rescue the bone loss caused by estrogen deficiency. To eliminate senescent cells in mice *in vivo*, we utilized an established transgenic mouse model that contains a 'suicide' transgene, called *INK-ATTAC*,[18] that permits the inducible elimination of $p16^{Ink4a}$-expressing senescent cells after dosing the mice with AP20187 (Note: the *INK-ATTAC* construct schematic and mechanism of apoptosis activation in $p16^{Ink4a}$-positive senescent cells upon administration of AP20187 to *INK-ATTAC* mice is shown in Supplementary Fig. 2). In our earlier work,[11] we randomized old female *INK-ATTAC* mice starting at 20 months of age that had established bone loss to either Vehicle or AP20187 treatments biweekly for four months. We found that systemic elimination of senescent cells in old female *INK-ATTAC* mice improved skeletal health at both the spine and femur, including increased BV/TV, Tb.N, Tb.Th, and decreased Tb.Sp as well as increased Ct.Th.[11] These data demonstrate that elimination of senescent cells in old female *INK-ATTAC* mice prevents age-related bone loss.[11] To determine whether systemic elimination of senescent cells protects against bone loss caused by estrogen deficiency, in the current study we randomized 51 young adult (4-month-old) female *INK-ATTAC* mice to SHAM+Vehicle (n=17), OVX+Vehicle (n=17), or OVX+AP20187 (n=17) for 8 weeks (Fig. 4A). As anticipated, uterine weights were significantly reduced (by 107–114%; $p < 0.001$) in both OVX groups relative to SHAM (Fig. 4B). Further, OVX in both groups caused significant weight gain (Fig. 4C), which resulted from increased fat mass (Fig. 4D) with no change in lean mass (Fig. 4E). We next assessed the skeletal phenotype of these animals using μCT. As depicted in Fig. 4F and quantified in Fig. 4G–J, OVX+Vehicle caused bone loss at the lumbar spine as compared to SHAM+Vehicle, including decreased BV/TV (−40%; $p < 0.001$), decreased Tb.N (−13%; $p < 0.001$), decreased Tb.Th (−13%; $p < 0.001$), and increased Tb.Sp (+12%; $p < 0.001$). In addition, estrogen deficiency caused significant loss of cortical bone at the femur in OVX+Vehicle mice relative to SHAM+Vehicle *INK-ATTAC* mice (Fig. 4K), due to cortical thinning (−7%; $p < 0.05$; Fig. 4L) resulting from endocortical resorption (+6%; $p < 0.05$; Fig. 4M) with no significant ($p > 0.05$) change in periosteal circumference (Fig. 4N). However, treatment of young adult estrogen deficient female *INK-ATTAC* mice with AP20187, which eliminates senescent cells and protects against age-related bone loss in old female *INK-ATTAC* mice,[11] did not rescue the OVX-induced bone loss at the either the spine (Fig. 4F–J) or femur (Fig. 4K–N) (all *p-values* > 0.05). Thus,

p16^{Ink4a}-senescent cells in young adult life do not contribute to the bone loss caused by estrogen deficiency.

We next aimed to more definitively establish whether estrogen deficiency induces cellular senescence in bone of young adult mice. Thus, in osteocyte-enriched bone samples isolated from the young adult female *INK-ATTAC* mice, we first used rt-qPCR to measure the mRNA expression of *EGFP*, which is encoded by the *INK-ATTAC* transgene,[18] thus permitting *in vivo* monitoring of *p16*^{Ink4a}-senescent cells. As evident in Fig. 5A, we found no changes (all *p-values* > 0.05) in *EGFP* levels in bone in response to either OVX+Vehicle or OVX+AP20187 relative to SHAM+Vehicle. In addition, we found no changes (all *p-values* > 0.05) in mRNA levels of endogenous *p16*^{Ink4a} (*Cdkn2a*; Fig. 5B), *p21*^{Cip1} (*Cdkn1a*; Fig. 5C), or *p53* (*Trp53*; Fig. 5D). Finally, we performed FISH on bone sections from the young adult *INK-ATTAC* mice coupled with confocal microscopy to measure an established senescence biomarker – *i.e.,* the SADS[13] assay (Fig. 5E). This analysis confirmed that estrogen deficiency alone (OVX+Vehicle) did not alter the percentage of senescent osteocytes in bone (*p-value* > 0.05 *versus* SHAM+Vehicle; Fig. 5F), and that treatment of the young adult female mice that underwent OVX with AP20187, which eliminates senescent cells in the *INK-ATTAC* transgenic background,[18] did not significantly change the percentage of senescent osteocytes in bone (*p-values* > 0.05 *versus* SHAM+Vehicle and OVX+Vehicle; Fig. 5F). Thus, ovariectomy in young adult female *INK-ATTAC* mice does not alter cellular senescence biomarkers in bone.

Discussion

The timing, context, and extent to which estrogen deficiency and fundamental aging mechanisms such as cellular senescence contribute to the pathogenesis of osteoporosis has been an important unanswered question in the fields of bone and mineral research and the biology of aging. While estrogen deficiency has undoubtedly been established as a seminal mechanism in the pathogenesis of osteoporosis,[1,2] the importance of cellular senescence as a causal mediator of age-related bone loss has become increasingly clear in recent years.[10,11,38,39]

Certain types of stress cause cellular senescence, which is an irreversible growth arrest cell fate characterized by upregulation of the senescence biomarker – *p16*^{Ink4a}. In addition, in specific contexts cellular senescence can be accompanied by increased expression of the cell cycle inhibitor *p21*^{Cip1}, which is downstream of p53. Emerging evidence has established that senescent cells accumulate naturally in various tissues with advancing age.[40] Bone is no exception to this phenomenon as findings from our group[10] as well as others[12,14] establish that with aging, a relatively small subpopulation of cells from various separate lineages within the bone microenvironment become senescent. It is noteworthy, however, that even in very old age, only a small subset of cells undergo senescence – *e.g.,* in mouse bone we found that ~11% of osteocytes become senescent with aging.[10] This is consistent with findings in adipose tissue of old mice showing that up to ~14% of cells become senescent,[41] while ~15% of fibroblasts in the skin of very old primates become senescent.[42] Notwithstanding, despite their relatively low abundance, senescent cells have profound

biological relevance and consequences in various old tissues as these cells have been implicated in driving several age-related chronic diseases.[9]

Indeed, in recent years several groups have shown that genetic or pharmacological selective elimination of senescent cells has a remarkable therapeutic impact across multiple organ systems in mouse models of aging and chronic pathological diseases, including metabolic dysfunction,[29] atherosclerosis/cardiovascular disease,[30,43] hepatic steatosis,[44] pulmonary fibrosis,[45] osteoarthritis,[46] and sarcopenia/frailty.[47] Furthermore, as noted earlier, our group has demonstrated that targeting senescent cells in old mice has beneficial effects on bone mass and microarchitecture with the beneficial effects of targeting senescent cells due to increased bone formation on endocortical surfaces and suppressed bone resorption.[11] These findings have not only led to a new potential avenue for treating osteoporotic patients that may offer advantages over conventional anti-resorptive therapy,[38,39] but also point to the potential path of targeting senescent cells therapeutically to extend healthspan – *i.e.,* the healthy period of life free of chronic diseases. However, in order to translate new drugs that target senescent cells (so-called “senotherapeutics”) to human trials, their efficacy and safety must first be tested in appropriate preclinical animal models.

Given that FDA guidelines for evaluation of osteoporosis drugs state that bone quality studies should be performed in ovariectomized animals,[7] in the current study we utilized multiple approaches in mice and humans to rigorously investigate a possible direct role for estrogen in the regulation of cellular senescence. We first studied both female and male WT mice that had undergone gonadectomy and found no evidence for increased cellular senescence in bone compared to sham-operated controls. Furthermore, our data indicate that acquisition of a distinctive pro-inflammatory secretory program (*i.e.,* the SASP), whereby senescent cells secrete a complex array of cytokines, chemokines, and matrix-degrading proteases,[15–17] develops with natural chronological aging in the bone microenvironment,[10] whereas by contrast sex steroid deficiency alone did not induce the SASP in bone. We then examined senescence and SASP markers in human bone biopsies obtained from older healthy postmenopausal women who received either no treatment or estrogen therapy for three weeks. Consistent with our findings in mice, we found no evidence of changes in senescence biomarkers or SASP factors in human bone in response to estrogen therapy. Nevertheless, it should be noted that previous studies in mice have observed changes in pro-inflammatory cytokines, some of which are part of the SASP, in the bone microenvironment in response to ovariectomy.[48–53] However, the timepoints considered by these studies and the sources of these pro-inflammatory cytokines were variable, which may at least in part explain why changes in these factors were not found in the present study.

Finally, we took advantage of a novel transgenic mouse model that permits the inducible (via the synthetic drug – AP20187) elimination of $p16^{Ink4a}$-senescent cells.[18] After randomizing sham-operated or ovariectomized female young adult *INK-ATTAC* mice to either vehicle or AP20187 treatments, we found that ovariectomy alone is not sufficient to induce cellular senescence in bone and that elimination of $p16^{Ink4a}$-senescent cells in young adult life does not restore the bone loss caused by estrogen deficiency. These findings can be explained by the low abundance of senescent cells during young adulthood, which was not changed by sex steroid deficiency; thus, we propose that elimination of this small naturally

occurring population of senescent cells had no overt effect. These findings are consistent with our previous work demonstrating treating young adult *INK-ATTAC* mice with AP20187 does not alter skeletal parameters,[11] establishing that this strategy is specific to the prevention of the bone loss that occurs in old age. Taken together with our previous *in vivo* findings that senescent cells accumulate in the bone microenvironment at the time and location of age-related bone loss in both mice and humans,[10] and that targeting senescence cells in mice by either their selective elimination or by inhibiting their SASP prevents age-related bone loss,[11] our collective data establish that estrogen deficiency and cellular senescence represent independent mechanisms in the pathogenesis of osteoporosis.

As noted earlier, we focused our animal studies on inducing sex steroid deficiency in young adulthood as FDA guidelines recommend ovariectomy as a standard preclinical animal model to demonstrate the efficacy and safety of new potential drugs for osteoporosis therapy.[7] However, because we studied young adult animals, we cannot exclude the possibility that there may be an interaction between cellular senescence and sex steroid deficiency specifically in the context of aging, although our findings in older postmenopausal women treated with estrogen therapy do not support such an interaction. Furthermore, we acknowledge that it is possible that in contrast to aging, in youth the immune system could be capable of rapidly clearing the senescent cells[54] caused by sex steroid deficiency that, although outside the scope of this current study, is an intriguing possibility that should be examined in the future. In addition, it is possible that in contrast to our findings in young adult mice, sex steroid deficiency may result in senescent cell accumulation in middle-aged mice, which should be tested in future studies. Interestingly, it appears that long-term estrogen deficiency in women who had ovariectomies as young adults can experience accelerated development of aging phenotypes once these women are much older.[24] Thus, it remains at least formally possible that estrogen deficiency over decades could turn out to be associated with an increase in senescent cell accumulation, a speculation that warrants further investigation. Finally, it will be interesting in future studies to establish whether accelerated cellular aging occurs with sex steroid deficiency as it relates to other hallmarks of skeletal aging,[8] including genomic instability (*e.g.,* impaired DNA repair) and mitochondrial dysfunction (*e.g.,* oxidative stress).

Notwithstanding, the findings from our study will impact how novel senotherapeutics, including senolytics (*i.e.*, drugs that selectively eliminate senescent cells) and senomorphics (*i.e.*, drugs that inhibit the SASP), will need to be tested for skeletal efficacy in preclinical studies. Indeed, these studies will be important in assessing potential toxicities and to identify, develop, and optimize senotherapeutic dosing regimens. This will be imperative toward potentially translating senotherapeutics as a class of drugs to the clinic.

Conclusions

In conclusion, our data establish that estrogen deficiency and cellular senescence represent independent mechanisms in the pathogenesis of osteoporosis. Moreover, these findings have important implications for testing novel senolytics and senomorphics for skeletal efficacy, as these drugs will need to be evaluated in preclinical models of aging, as opposed to the current FDA model of prevention of ovariectomy-induced bone loss.

Supplementary Material

Refer to Web version on PubMed Central for supplementary material.

Acknowledgements

This work was supported by National Institutes of Health (NIH) grants AR070241 (J.N.F.), AG004875 (S.K.), AG048792 (S.K.), AR068275 (D.G.M.), AG013925 (J.L.K.), AG049182 (J.L.K.), the Connor Group (J.L.K), Robert J. and Theresa W. Ryan (J.L.K), the Noaber and Ted Nash Long Life Foundations (J.L.K.), and both a High-Risk Pilot Award (J.N.F. and S.K.) and a Career Development Award (J.N.F.) from the Mayo Clinic Robert and Arlene Kogod Center on Aging, as well as the Richard F. Emslander Career Development Award in Endocrinology (J.N.F.).

References

1. Khosla S, Monroe DG. Regulation of Bone Metabolism by Sex Steroids. Cold Spring Harb Perspect Med 2018;8(1).
2. Almeida M, Laurent MR, Dubois V, et al. Estrogens and Androgens in Skeletal Physiology and Pathophysiology. Physiol Rev 2017;97(1):135–87. [PubMed: 27807202]
3. Albright F Post-menopausal osteoporosis. Trans Assoc Am Physicians 1940;55:298–305.
4. Rossouw JE, Anderson GL, Prentice RL, et al. Risks and benefits of estrogen plus progestin in healthy postmenopausal women: principal results from the Women's Health Initiative randomized controlled trial. Jama 2002;288(3):321–33. [PubMed: 12117397]
5. Parente L, Uyehara C, Larsen W, Whitcomb B, Farley J. Long-term impact of the women's health initiative on HRT. Arch Gynecol Obstet 2008;277(3):219–24. [PubMed: 17713777]
6. Khosla S Update on Estrogens and the skeleton. J Clin Endocrinol Metab 2010;95:3569–77. [PubMed: 20685883]
7. US Food and Drug Administration. Osteoporosis: Nonclinical Evalulation of Drugs Intended for Treatment Access Date: 11/13/2018 Web Page: www.fda.gov/downloads/Drugs/GuidanceComplianceRegulatoryInformation/Guidances/UCM506366.pdf.
8. Farr JN, Almeida M. The Spectrum of Fundamental Basic Science Discoveries Contributing to Organismal Aging. J Bone Miner Res 2018;33(9):1568–84. [PubMed: 30075061]
9. Tchkonia T, Zhu Y, van Deursen J, Campisi J, Kirkland JL. Cellular senescence and the senescent secretory phenotype: therapeutic opportunities. J Clin Invest 2013;123(3):966–72. [PubMed: 23454759]
10. Farr JN, Fraser DG, Wang H, et al. Identification of Senescent Cells in the Bone Microenvironment. J Bone Miner Res 2016;31(11):1920–9. [PubMed: 27341653]
11. Farr JN, Xu M, Weivoda MM, et al. Targeting cellular senescence prevents age-related bone loss in mice. Nat Med 2017;23(9):1072–9. [PubMed: 28825716]
12. Piemontese M, Almeida M, Robling AG, et al. Old age causes de novo intracortical bone remodeling and porosity in mice. JCI Insight 2017;2(17).
13. Swanson EC, Manning B, Zhang H, Lawrence JB. Higher-order unfolding of satellite heterochromatin is a consistent and early event in cell senescence. J Cell Biol 2013;203(6):929–42. [PubMed: 24344186]
14. Kim HN, Chang J, Shao L, et al. DNA damage and senescence in osteoprogenitors expressing Osx1 may cause their decrease with age. Aging Cell 2017;16(4):693–703. [PubMed: 28401730]
15. Coppe JP, Patil CK, Rodier F, et al. Senescence-associated secretory phenotypes reveal cell-nonautonomous functions of oncogenic RAS and the p53 tumor suppressor. PLoS Biol 2008;6(12):2853–68. [PubMed: 19053174]
16. Acosta JC, Banito A, Wuestefeld T, et al. A complex secretory program orchestrated by the inflammasome controls paracrine senescence. Nat Cell Biol 2013;15(8):978–90. [PubMed: 23770676]
17. Coppe JP, Desprez PY, Krtolica A, Campisi J. The senescence-associated secretory phenotype: the dark side of tumor suppression. Annu Rev Pathol 2010;5:99–118. [PubMed: 20078217]

18. Baker DJ, Wijshake T, Tchkonia T, et al. Clearance of p16Ink4a-positive senescent cells delay aging-associated disorders. Nature 2011;479(7372):232–6. [PubMed: 22048312]
19. Zhu Y, Tchkonia T, Pirtskhalava T, et al. The Achilles' heel of senescent cells: from transcriptome to senolytic drugs. Aging Cell 2015;14(4):644–58. [PubMed: 25754370]
20. Xu M, Tchkonia T, Ding H, et al. JAK inhibition alleviates the cellular senescence-associated secretory phenotype and frailty in old age. Proc Natl Acad Sci U S A 2015;112(46):E6301–10. [PubMed: 26578790]
21. Colman EG. The Food and Drug Administration's Osteoporosis Guidance Document: past, present, and future. J Bone Miner Res 2003;18(6):1125–8. [PubMed: 12817768]
22. Rocca WA, Gazzuola-Rocca L, Smith CY, et al. Accelerated Accumulation of Multimorbidity After Bilateral Oophorectomy: A Population-Based Cohort Study. Mayo Clinic proceedings 2016;91(11):1577–89. [PubMed: 27693001]
23. Rocca WA, Gazzuola Rocca L, Smith CY, et al. Bilateral Oophorectomy and Accelerated Aging: Cause or Effect? J Gerontol A Biol Sci Med Sci 2017;72(9):1213–7. [PubMed: 28329133]
24. Rocca WA, Gazzuola Rocca L, Smith CY, et al. Loss of Ovarian Hormones and Accelerated Somatic and Mental Aging. Physiology (Bethesda) 2018;33(6):374–83. [PubMed: 30303778]
25. Lopez-Otin C, Blasco MA, Partridge L, Serrano M, Kroemer G. The hallmarks of aging. Cell 2013;153(6):1194–217. [PubMed: 23746838]
26. Fujita K, Roforth MM, Demaray S, et al. Effects of estrogen on bone mRNA levels of sclerostin and other genes relevant to bone metabolism in postmenopausal women. J Clin Endocrinol Metab 2014;99(1):E81–8. [PubMed: 24170101]
27. Roforth MM, Fujita K, McGregor UI, et al. Effects of age on bone mRNA levels of sclerostin and other genes relevant to bone metabolism in humans. Bone 2014;59:1–6. [PubMed: 24184314]
28. Farr JN, Roforth MM, Fujita K, et al. Effects of Age and Estrogen on Skeletal Gene Expression in Humans as Assessed by RNA Sequencing. PLoS One 2015;10(9):e0138347. [PubMed: 26402159]
29. Xu M, Palmer AK, Ding H, et al. Targeting senescent cells enhances adipogenesis and metabolic function in old age. Elife 2015;4:e12997. [PubMed: 26687007]
30. Roos CM, Zhang B, Palmer AK, et al. Chronic senolytic treatment alleviates established vasomotor dysfunction in aged or atherosclerotic mice. Aging Cell 2016;15(5):973–7. [PubMed: 26864908]
31. Schafer MJ, White TA, Evans G, et al. Exercise Prevents Diet-Induced Cellular Senescence in Adipose Tissue. Diabetes 2016;65(6):1606–15. [PubMed: 26983960]
32. Radonic A, Thulke S, Mackay IM, et al. Guideline to reference gene selection for quantitative real-time PCR. Biochem Biophys Res Commun 2004;313:856–62. [PubMed: 14706621]
33. Vandesompele J, De Preter K, Pattyn F, et al. Accurate normalization of real-time quantitative RT-PCR data by geometeric averaging of multiple internal control genes. Genome Biol 2002;3:research0034.1-0-34.11.
34. Zhao S, Fernald RD. Comprehensive algorithm for quantitative real-time polymerase chain reaction. J Comput Biol 2005;12(8):1047–64. [PubMed: 16241897]
35. Fujita K, Roforth MM, Atkinson EJ, et al. Isolation and characterization of human osteoblasts from needle biopsies without in vitro culture. Osteoporos Int 2014;25(3):887–95. [PubMed: 24114401]
36. Subramanian A, Tamayo P, Mootha VK, et al. Gene set enrichment analysis: a knowledge-based approach for interpreting genome-wide experssion profiles. Proc Natl Acad Sci USA 2005;102:15545–50. [PubMed: 16199517]
37. Efron B, Tibshirani R. On testing the significance of sets of genes. Ann Appl Statist 2007;1(1): 107–29.
38. Khosla S, Farr JN, Kirkland JL. Inhibiting Cellular Senescence: A New Therapeutic Paradigm for Age-Related Osteoporosis. J Clin Endocrinol Metab 2018.
39. Farr JN, Khosla S. Cellular senescence in bone. Bone 2019;121:121–33. [PubMed: 30659978]
40. Krishnamurthy J, Torrice C, Ramsey MR, et al. Ink4a/Arf expression is a biomarker of aging. J Clin Invest 2004;114(9):1299–307. [PubMed: 15520862]
41. Biran A, Zada L, Abou Karam P, et al. Quantitative identification of senescent cells in aging and disease. Aging Cell 2017;16(4):661–71. [PubMed: 28455874]

42. Herbig U, Ferreira M, Condel L, Carey D, Sedivy JM. Cellular senescence in aging primates. Science 2006;311:1257. [PubMed: 16456035]
43. Childs BG, Baker DJ, Wijshake T, et al. Senescent intimal foam cells are deleterious at all stages of atherosclerosis. Science 2016;354(6311):472–7. [PubMed: 27789842]
44. Ogrodnik M, Miwa S, Tchkonia T, et al. Cellular senescence drives age-dependent hepatic steatosis. Nat Commun 2017;8:15691. [PubMed: 28608850]
45. Schafer MJ, White TA, Iijima K, et al. Cellular senescence mediates fibrotic pulmonary disease. Nat Commun 2017;8:14532. [PubMed: 28230051]
46. Jeon OH, Kim C, Laberge RM, et al. Local clearance of senescent cells attenuates the development of post-traumatic osteoarthritis and creates a pro-regenerative environment. Nat Med 2017;23(6): 775–81. [PubMed: 28436958]
47. Xu M, Pirtskhalava T, Farr JN, et al. Senolytics improve physical function and increase lifespan in old age. Nat Med 2018;24(8):1246–56. [PubMed: 29988130]
48. Jilka RL, Hangoc G, Girasole G, et al. Increased osteoclast development after estrogen loss: Mediation by interleukin-6. Science 1992;257:88–91. [PubMed: 1621100]
49. Cenci S, Weitzmann MN, Roggia C, et al. Estrogen deficiency induces bone loss by enhancing T-cell production of TNF-alpha. J Clin Invest 2000;106:1229–37. [PubMed: 11086024]
50. Roggia C, Gao Y, Cenci S, et al. Up-regulation of TNF-producing T cells in the bone marrow: a key mechanism by which estrogen deficiency induces bone loss in vivo. Proc Natl Acad Sci U S A 2001;98(24):13960–5. [PubMed: 11717453]
51. Cenci S, Toraldo G, Weitzmann MN, et al. Estrogen deficiency induces bone loss by increasing T cell proliferation and lifespan through IFN-gamma-induced class II transactivator. Proc Natl Acad Sci USA 2003;100(18):10405–10. [PubMed: 12923292]
52. Weitzmann MN, Pacifici R. Estrogen deficiency and bone loss: an inflammatory tale. J Clin Invest 2006;116:1186–94. [PubMed: 16670759]
53. Straub RH. The complex role of estrogens in inflammation. Endocr Rev 2007;28:521–71. [PubMed: 17640948]
54. Wang J, Geiger H, Rudolph KL. Immunoaging induced by hematopoietic stem cell aging. Curr Opin Immunol 2011;23(4):532–6. [PubMed: 21872769]

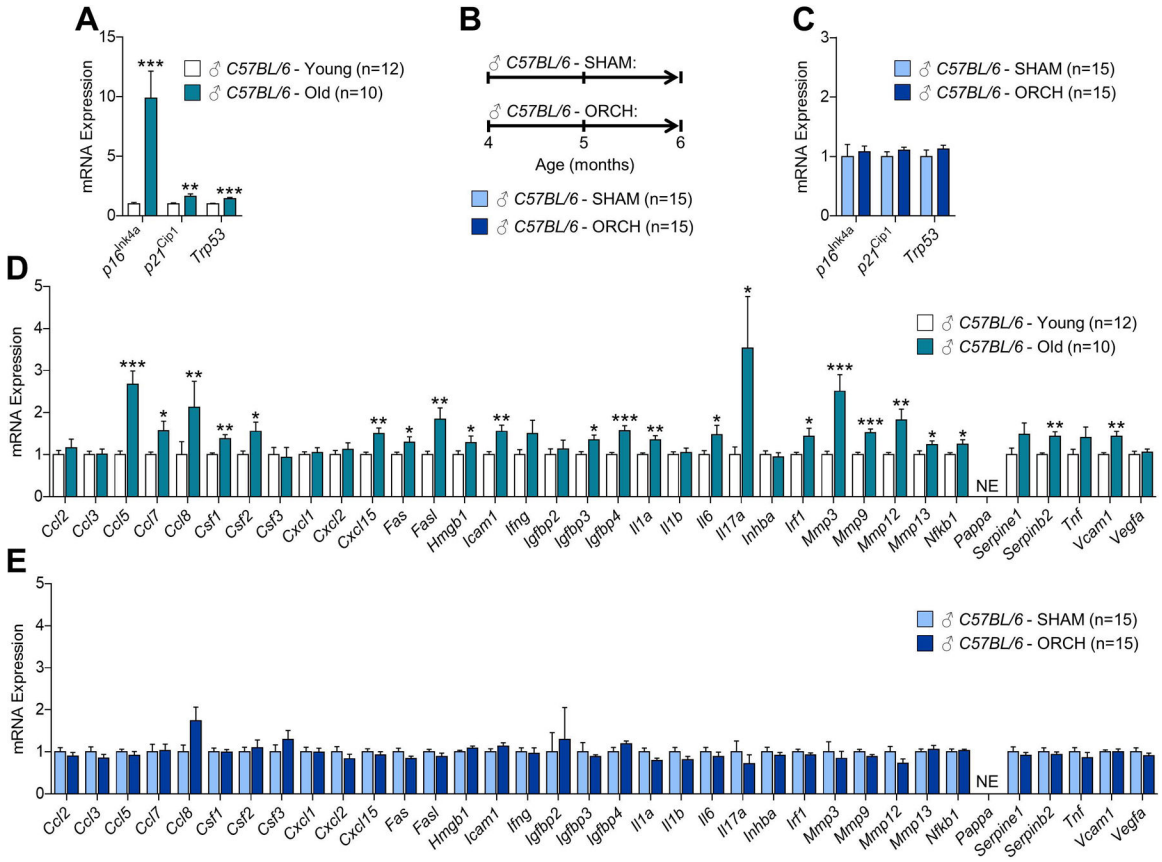

Fig 1. Comparisons of changes in senescence biomarkers and senescence-associated secretory phenotype (SASP) factors in osteocyte-enriched bone samples from male mice in the context of natural chronological aging and sex steroid deficiency.

(*A*) rt-qPCR analysis of *in vivo* age-associated changes in mRNA expression of the senescence effectors, $p16^{Ink4a}$ (*Cdkn2a*), $p21^{Cip1}$ (*Cdkn1a*), and *p53* (*Trp53*), in osteocyte-enriched bone samples from young (6-month-old, n=12) *versus* old (24-month-old, n=10) male *C57BL/6* wild-type (WT) mice (data reproduced from *J Bone Miner Res* 31(11):1920–9, 2016). (*B*) Experimental design for testing the effects of orchidectomy-induced sex steroid deficiency on biomarkers of cellular senescence in bone; 4-month-old male C57BL/6 WT mice were randomized to undergoing either sham surgery (SHAM, n=15) or orchidectomy (ORCH, n=15) for 2 months; all animals were sacrificed at age 6 months. (*C*) rt-qPCR analysis of *in vivo* changes in mRNA expression of the senescence effectors, $p16^{Ink4a}$ (*Cdkn2a*), $p21^{Cip1}$ (*Cdkn1a*), and *p53* (*Trp53*), in osteocyte-enriched bone samples from SHAM (n=15) *versus* ORCH (n=15) male *C57BL/6* WT mice. (*D*) rt-qPCR analysis of *in vivo* age-associated changes in mRNA expression of 36 established SASP factors in osteocyte-enriched bone samples from young (6-month-old, n=12) *versus* old (24-month-old, n=10) male *C57BL/6* WT mice (data reproduced from *J Bone Miner Res* 31(11):1920–9, 2016). (*E*) rt-qPCR analysis of *in vivo* changes in mRNA expression of 36 established SASP factors in osteocyte-enriched bone samples from SHAM (n=15) *versus* ORCH (n=15) male *C57BL/6* WT mice. Data represent mean ± SEM (error bars); NE = Not expressed (Cycle threshold [Ct] values >35). *$p < 0.05$; **$p < 0.01$; ***$p < 0.001$ (independent samples *t*-test).

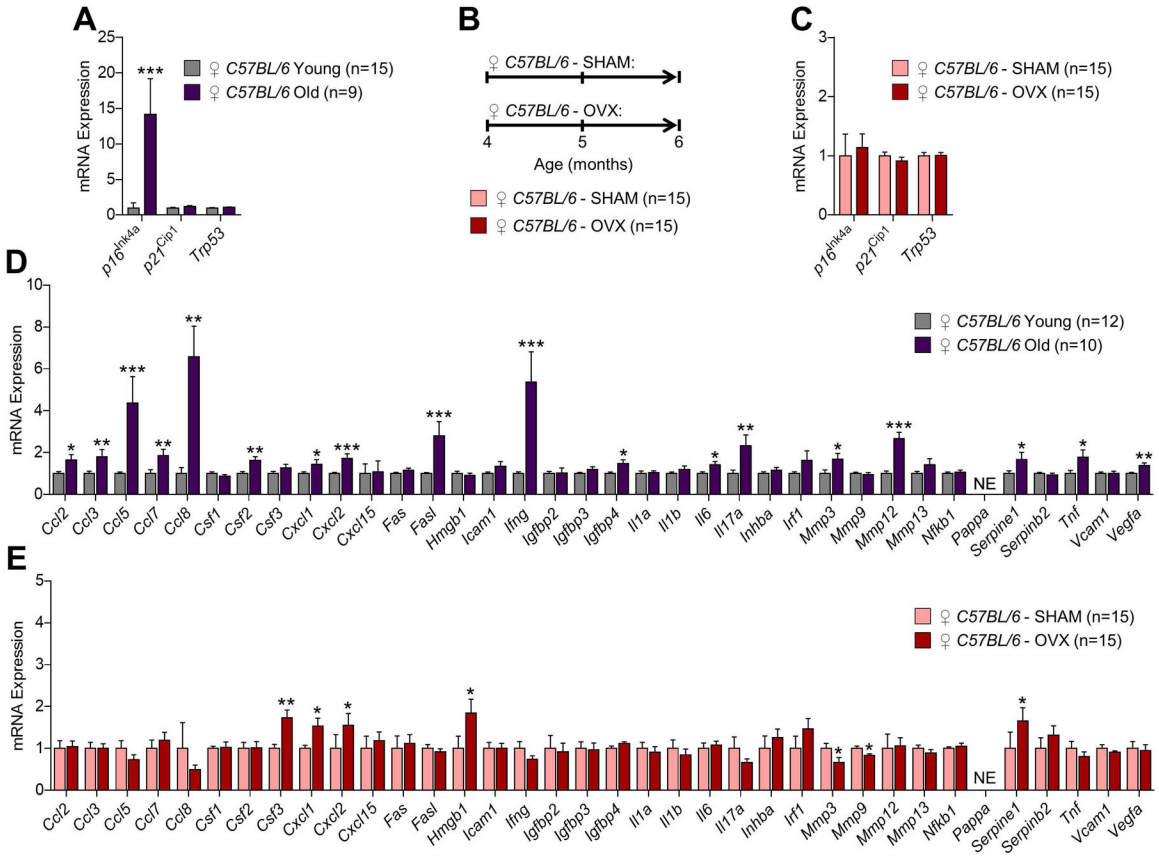

Fig 2. Comparisons of changes in senescence biomarkers and senescence-associated secretory phenotype (SASP) factors in osteocyte-enriched bone samples from female mice in the context of natural chronological aging and sex steroid deficiency.

(*A*) rt-qPCR analysis of *in vivo* age-associated changes in mRNA expression of the senescence effectors, $p16^{Ink4a}$ (*Cdkn2a*), $p21^{Cip1}$ (*Cdkn1a*), and *p53* (*Trp53*), in osteocyte-enriched bone samples from young (6-month-old, n=15) *versus* old (24-month-old, n=9) female *C57BL/6* wild-type (WT) mice (data reproduced from *J Bone Miner Res* 31(11): 1920–9, 2016). (*B*) Experimental design for testing the effects of ovariectomy-induced sex steroid deficiency on biomarkers of cellular senescence in bone; 4-month-old female C57BL/6 WT mice were randomized to undergoing either sham surgery (SHAM, n=15) or ovariectomy (OVX, n=15) for 2 months; all animals were sacrificed at age 6 months. (*C*) rt-qPCR analysis of *in vivo* changes in mRNA expression of the senescence effectors, $p16^{Ink4a}$ (*Cdkn2a*), $p21^{Cip1}$ (*Cdkn1a*), and *p53* (*Trp53*), in osteocyte-enriched bone samples from SHAM (n=15) *versus* OVX (n=15) female *C57BL/6* WT mice. (*D*) rt-qPCR analysis of *in vivo* age-associated changes in mRNA expression of 36 established SASP factors in osteocyte-enriched bone samples from young (6-month-old, n=15) *versus* old (24-month-old, n=9) female *C57BL/6* WT mice. (*E*) rt-qPCR analysis of *in vivo* changes in mRNA expression of 36 established SASP factors in osteocyte-enriched bone samples from SHAM (n=15) *versus* OVX (n=15) female *C57BL/6* WT mice. Data represent mean ± SEM (error bars); NE = Not expressed (Cycle threshold [Ct] values >35). *$p < 0.05$; **$p < 0.01$; ***$p < 0.001$ (independent samples *t*-test).

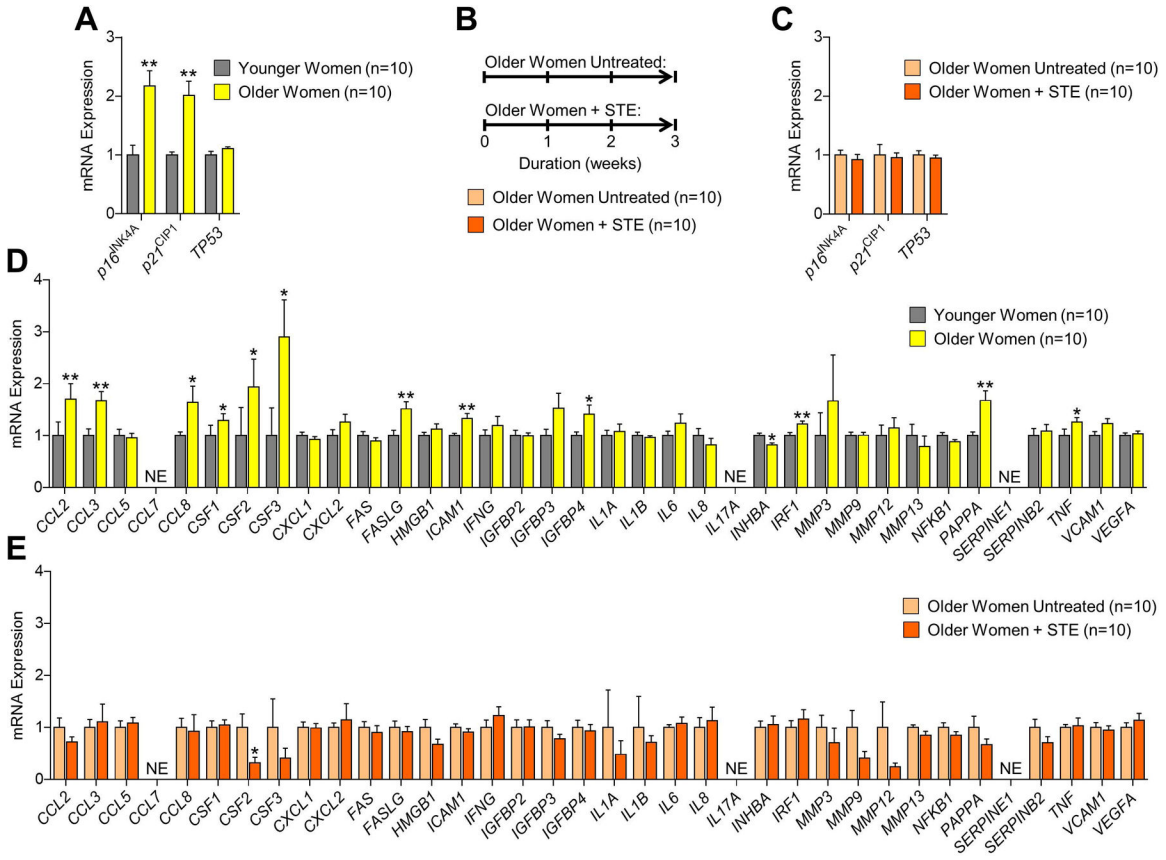

Fig. 3. Comparisons of changes in senescence biomarkers and senescence-associated secretory phenotype (SASP) factors in human bone biopsies obtained from healthy women in the context of aging and in response to short-term estrogen (STE) therapy.

(*A*) rt-qPCR analysis of *in vivo* age-associated changes in mRNA expression of the senescence effectors, $p16^{INK4A}$ (*CDKN2A*), $p21^{CIP1}$ (*CDKN1A*), and *p53* (*TP53*), in human bone biopsies isolated from healthy younger premenopausal (n=10; mean age ± SD, 27±3 yrs) *versus* healthy older postmenopausal (n=10; mean age ± SD, 78±5 yrs) women (data reproduced from *J Bone Miner Res* 31(11):1920–9, 2016). (*B*) Experimental design for testing the effects of STE therapy on biomarkers of cellular senescence in bone; human bone biopsies were obtained from 20 healthy postmenopausal women who received either no treatment (NT, n=10; mean age ± SD, 78±5 yrs) or short-term estrogen (STE, n=10; mean age ± SD, 74±5 yrs) therapy for 3 weeks. (*C*) rt-qPCR analysis of *in vivo* changes in mRNA expression of the senescence effectors, $p16^{INK4A}$ (*CDKN2A*), $p21^{CIP1}$ (*CDKN1A*), and p53 (*TP53*), in human bone biopsies isolated from 20 healthy postmenopausal women following either NT or STE therapy for 3 weeks. (*D*) rt-qPCR analysis of *in vivo* age-associated changes in mRNA expression of 36 established SASP factors in human bone biopsies isolated from younger premenopausal *versus* older postmenopausal women who received NT (data reproduced from *J Bone Miner Res* 31(11):1920–9, 2016). (*E*) rt-qPCR analysis of *in vivo* changes in mRNA expression of 36 established SASP factors in human bone biopsies isolated from 20 healthy postmenopausal women following either NT or STE therapy for 3 weeks. Data represent mean ± SEM (error bars); NE = Not expressed (Cycle

threshold [Ct] values >35). *$p < 0.05$; **$p < 0.01$; ***$p < 0.001$ (independent samples t-test).

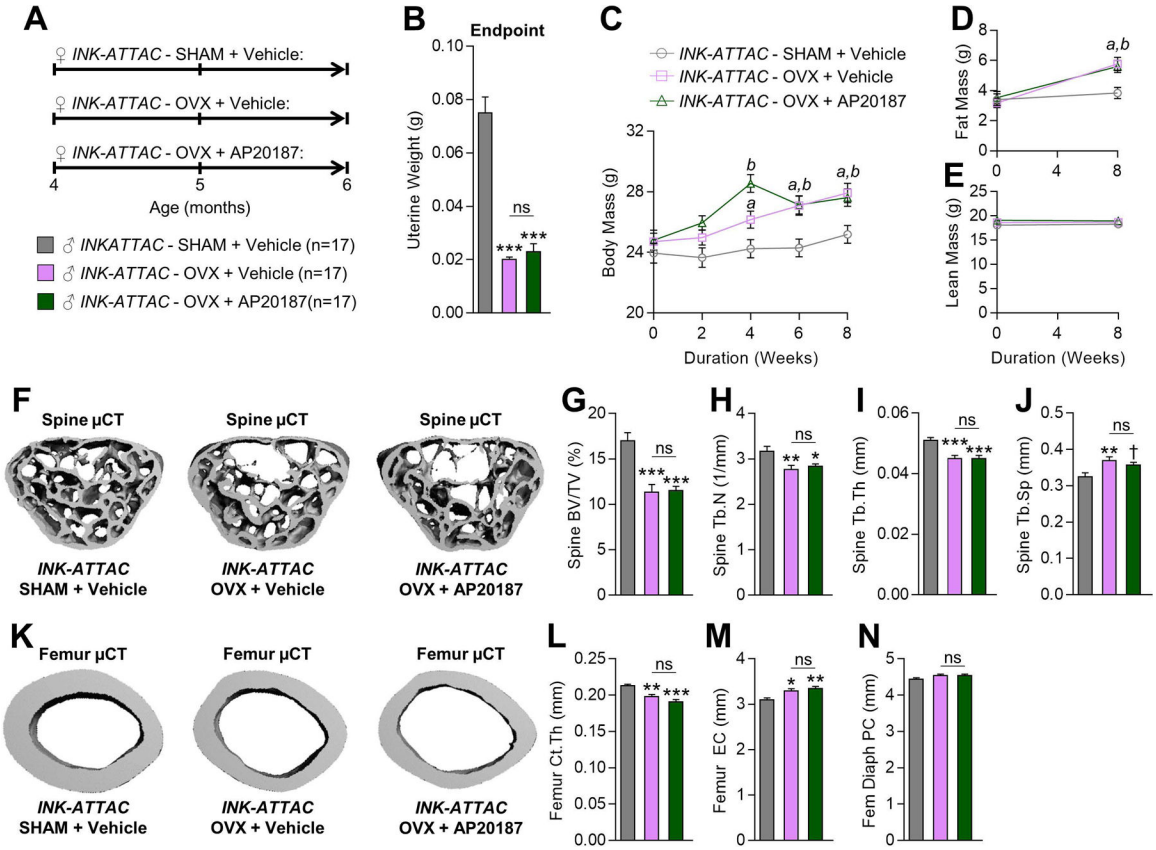

Fig. 4. Treatment with AP20187, which eliminates senescent cells in old *INK-ATTAC* mice, does not rescue ovariectomy (OVX)-induced bone loss in young mice.

(*A*) Experimental design for testing the effects of AP20187 treatment on OVX-induced bone loss; 4-month-old (Baseline) female *INK-ATTAC* mice were randomized to either SHAM +Vehicle (n=17), OVX+Vehicle (n=17), or OVX+AP20187 (n=17) for 8 weeks; all mice were sacrificed at age 6 months (Endpoint). Uterine weights (g) at study Endpoint in *INK-ATTAC* SHAM+Vehicle (n=17), *INK-ATTAC* OVX+Vehicle (n=17), and *INK-ATTAC* OVX +AP20187 mice. (*C*) Changes in total body mass (g) throughout the duration of the 8 wk study. (D) Changes in fat mass (g) from Baseline to study Endpoint. (*E*) Changes in lean mass (g) from Baseline to study Endpoint. (*F*) Representative micro-computed tomography (µCT) images of bone microarchitecture at the lumbar spine of *INK-ATTAC* SHAM +Vehicle (n=17), *INK-ATTAC* OVX+Vehicle (n=17), and *INK-ATTAC* OVX+AP20187 (n=17) mice. (*G–J*) Quantification of µCT-derived bone volume fraction (BV/TV; %) (*G*), trabecular number (Tb.N; 1/mm) (*H*), trabecular thickness (Tb.Th; mm) (*I*), and trabecular separation (Tb.Sp; mm) (*J*) at the lumbar spine. (*K*) Representative µCT images of bone microarchitecture at the femur diaphysis of *INK-ATTAC* SHAM+Vehicle (n=17), *INK-ATTAC* OVX+Vehicle (n=17), and *INK-ATTAC* OVX+AP20187 (n=17) mice. (*L–N*) Quantification of µCT-derived cortical thickness (Ct.Th; mm) (*L*), endocortical circumference (EC; mm) (*M*), and periosteal circumference (PC; mm) (*N*) at the femur diaphysis. (*O–P*) Quantification of plasma levels of markers of bone formation (amino-terminal propeptide of type I collagen [P1NP]) (*O*) and bone resorption (cross-linked C-telopeptide of type I collagen [CTx]) (*P*) in *INK-ATTAC* SHAM+Vehicle (n=17), *INK-*

ATTAC OVX+Vehicle (n=17), and *INK-ATTAC* OVX+AP20187 (n=17) mice at study Endpoint. Data represent mean ± SEM (error bars); ns = not significant ($p > 0.05$). *$p < 0.05$; **$p < 0.01$; ***$p < 0.001$ (one-way analysis of variance [ANOVA] followed by Tukey *post-hoc* test to adjust for multiple comparisons). $^{a}p < 0.05$ vs OVX+Vehicle vs SHAM +Vehicle (repeated measures ANOVA, followed by the Tukey *post-hoc* test to adjust for multiple comparisons); $^{b}p < 0.05$ vs OVX+Vehicle vs SHAM+Vehicle (repeated measures ANOVA, followed by the Tukey *post-hoc* test to adjust for multiple comparisons).

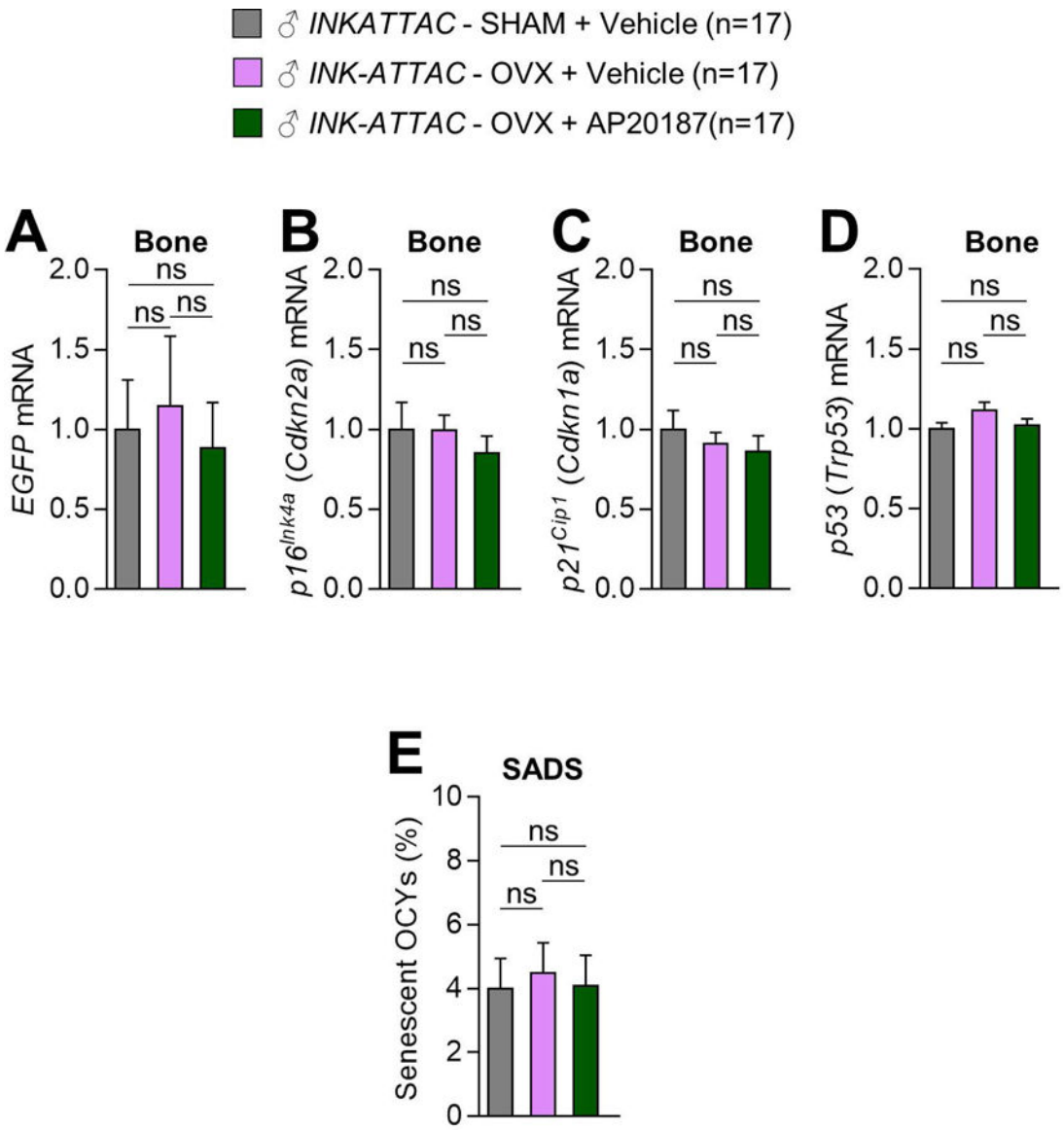

Fig. 5. Treatment with AP20187 in young female *INK-ATTAC* mice does not alter senescence biomarkers in bone following OVX.

(*A–D*) rt-qPCR analysis of *in vivo* changes in mRNA expression of enhanced green fluorescent protein (*EGFP*) (*A*), which is encoded by the *INK-ATTAC* transgene, as well as the senescence effectors, $p16^{Ink4a}$ (*Cdkn2a*) (*B*), $p21^{Cip1}$ (*Cdkn1a*) (*C*), and *p53* (*Trp53*) (*D*), in osteocyte-enriched samples from 6-month-old female *INK-ATTAC* SHAM+Vehicle (n=17), *INK-ATTAC* OVX+Vehicle (n=17), and *INK-ATTAC* OVX+AP20187 (n=17) mice (see experimental design in Fig. 4A). (*E*) Quantification of the percentage of senescent osteocytes (OCYs) in 6-month-old female *INK-ATTAC* SHAM+Vehicle (n=17), *INK-ATTAC* OVX+Vehicle (n=17), and *INK-ATTAC* OVX+AP20187 (n=17) mice according to the SADS assay performed on cortical bone diaphyses (n > 30 images per animal, n=8 mice/group). Data represent mean ± SEM (error bars); ns = not significant ($p > 0.05$; one-way

analysis of variance [ANOVA] followed by Tukey *post-hoc* test to adjust for multiple comparisons).